Am J Transl Res 2015;7(12):2612-2629
www.ajtr.org /ISSN:1943-8141/AJTR0015271

Original Article

A novel method in preparation of acellularporcine corneal stroma tissue for lamellar keratoplasty

Yi Shao[1,2,3], Jing Tang[1], Yueping Zhou[1,3], Yangluowa Qu[1,3], Hui He[1,3], Qiuping Liu[1,4], Gang Tan[5], Wei Li[1,3], Zuguo Liu[1,3]

[1]Eye Institute & Affiliated Xiamen Eye Center of Xiamen University, Xiamen, Fujian 361005, China; [2]Department of Ophthalmology, The First Affiliated Hospital of Nanchang University, Jiangxi Province Clinical Ophthalmology Institute, Nanchang, Jiangxi 330006, China; [3]Fujian Provincial Key Laboratory of Ophthalmology and Visual Science, Xiamen, Fujian 361005, China; [4]Department of Ophthalmology, The First Hospital of Xi'an City, Xi'an, Shanxi 710000, China; [5]Department of Ophthalmology, The First Affiliated Hospital of Nanhua University, Hengyang, Hunan 421000, China

Received August 29, 2015; Accepted December 13, 2015; Epub December 15, 2015; Published December 30, 2015

Abstract: Our objective was to develop a novel lamellar cornealbiomaterial for corneal reconstruction.Theporcine acellular corneal stroma discs (ACSDs) were prepared from de-epithelized fresh porcine corneas (DFPCs) by incubation with 100% fresh human serum and additional electrophoresis at 4°C. Such manipulation removed theanterior corneal stromal cells without residual of DNA content and α-Galantigen.Human serum decellularizing activity on porcineanterior corneal stroma cells is through apoptosis, and associated with the presence of α-Gal epitopes in anterior stroma. ACSDs displayed similar optical, biomechanical properties and ultrastructure to DFPCs, and showed good histocompatibility in rabbit corneal stromal pockets and anterior chamber. Rabbit corneallamellar keratoplasty (LKP) using ACSDs showed no rejection and high transparency of cornea at 2 months after surgery. In vivo confocal laser scanning microscopy and immunostaining analysis showed complete re-epithelization and stromal cell in growth of ACSDs without inflammatory cell infiltration, new blood vessel ingrowth and excessive wound healing. In conclusion, this novel decellularization method may be valuable for preparation of xenogenic corneal tissue for clinical application, ACSDs resulted from this method may be served as a matrix equivalent for LKP in corneal xenotransplantation.

Keywords: Corneal tissue engineering, xenotransplantation, human serum, α-gal, decellularization, ACSDs

Introduction

The cornea is an avascular, transparent, and immune privileged tissue. Neovascularization and stromal scaring, resulting from corneal trauma, ulcer, chemical/thermal burn, usually leads to visual impairment or blindness [1]. At present, the only therapeutic option for vision restoration in these corneal traumas is lamella or penetrating keratoplasty [2]. However, the global shortage of donor tissue, particularly in Asian countries, circumscribes clinical application of these surgeries; as a result, a huge number of patients remain on the waiting list for corneal transplantation. To solve this problem, several groups have tried to produce corneal substitutes using cultured cells and extracellular matrix components [3-8] or biomaterials such as composite, natural and synthetic polymers [9-14]. To date, however, there has been no clinical trial testing the feasibility of these corneal substitutes.

In recent years, porcine organs have attracted much attention due to their potential application as alternative sources for xenotransplantation [15, 16]. Porcine cornea is of particular interest due to its similarity to human cornea in thickness, topography and stable refractive status [17, 18]. It is also readily available. The major obstacle that prevents porcine to human xenotransplantation is the xenogenic rejection of donor tissues [19]. Intensive studies have shown that xenogenic transplantation of vascularized tissues can cause hyperacute rejection, and that this rejection is mainly mediated by α-gal epitope expressed on donor cells [20].

The α-gal epitope is one of the most abundant carbohydrate epitopes on cells of non-primate mammals and New World monkeys, while it is absent in humans, apes and Old World monkeys. However, gastrointestinal bacteria can stimulate constant production of the specific anti-Gal antibody in humans, constituting about 1% of circulating immunoglobulins [21]. Anti-Gal mediates the rejection of porcine organs in humans by bindingα-galepitopes in porcine endothelium and inducing complement-mediated destruction and antibody-dependent, cell-mediated destruction [22-24]. Different studies have shownthat α-gal epitopes are expressed in keratocytes of the anterior corneal stroma, but not in the epithelium or endothelium of porcine cornea [25-27], while the expression of α-gal epitopes will be enhanced in all corneal cells after xenogenic corneal transplantation [25]. Xenotransplantation of porcine cornea to other species such as rabbits, rats, mice, or monkeys can cause acute rejection [28] or mild cellular rejection [27]; it is well accepted, therefore, that the α-gal epitope is the key factor that induces xeno-related corneal rejection [26].

In order to reduce antigenicity of the porcine cornea, a variety of approaches have been developed to eliminate corneal cells and create an acellular matrix using hypertonic saline [29, 30], N2 gas [4], detergent [2], or phospholipase A2 treatment [31]. Porcine to rabbit xenotransplantation experiments using an acellular matrix generated from the above-mentioned methods showed prominent results. However, there are no studies that evaluate the expression of α-gal epitopes after these decellularization methods.

In this study, we investigated a novel decellularization method by incubating de-epithelized fresh porcine corneas (DFPCs) with 100% fresh human serum and additional electrophoresis. The acellular corneal stromal discs (ACSDs) generated from this method were evaluated in terms of physical and biomechanical properties, ultrastructure, and antigenicity; the bio-compatibility of ACSDs was determined by in vivo xenotransplantation in rabbits. We found that such manipulation can remove stromal cells as well as α-gal epitopes from anterior porcine corneal stroma. The stromal scaffold developed from this procedure may be feasible for corneal lamellar transplantation.

Materials and methods

Special materials

The following special agents were used: TUNEL kit (Promega, USA); mouse anti-α-smooth muscle actin (α-SMA) monoclonal antibody (Abcam Biotechnology, UK); mouse anti-vimentin monoclonal antibody (Santa Cruz, USA); Alexa Fluor 568 conjugated Griffonia simplicifolia I isolectin B4 (GSIB4) (Invitrogen, USA); DAPI (Vector Laboratories, USA).

Preparation of fresh human serum

All studies using human tissues were in accordance with the tenets of the Declaration of Helsinki and the policies of the institutional review board for human subjects from Xiamen Eye Center (Xiamen, China). Under aseptic conditions,ninety milliliters of human blood was collected from healthy volunteers and centrifuged at 2000 rpm for 10 min. The supernatant serum was then harvested and stored in -20°C before use. Serumfrom blood hemotype A was applied in this study.

Preparation of porcinecorneal tissues

Porcine eyes (three months, either gender) were enucleated immediately after sacrifice and kept at 4°C in a moist chamber for less than 2 h before experimentation. The eyes had integral ocular surfaces with central corneal thickness (CCT) of 800-1000 μm, as measured by an ultrasound biomicroscopy (UBM, Suowei Corporation, China). After immersion in 0.25% povidone iodine solution for 10 min and rinsing 3 times with phosphate buffer saline (PBS, pH 7.4) for 30 min, the porcine cornea was removed with scissors. The corneal epithelium and endothelium was then removed with a cell scraper, and the central corneal stroma was cut by trephine in different diameters. After that, the central corneas were further dissected manually to separate the anterior, middle, and deep stromal lamellar tissues, about 300 μm in thickness, respectively [32]. Anterior stromal lamellar tissue generated from such manipulation was defined as DFPCs.

Decellularization of porcine corneal tissues

Full thickness porcine corneasor stromal lamellar tissues (with or without epithelium) were

incubated in 100% sterile human serum or PBS at 37°C for durations up to 24 h. To observe the cellular nuclei, these tissues above were stained with DAPI. After rinsing with PBS 3 times for 20 min, some DFPCs were subjected to electrophoresis (150 V/cm) in a sterilized buffer (pH 7.4, 320 mosmol/kg) containing 40 mM Tris-base, 18 mM glacial acetic acid, and antibiotics (100 IU/ml penicillin, 100 mg/ml streptomycin and 0.625 mg/ml amphotericin) for 1 h at 4°C; this was followed by 3 washes with PBS for 20 min at 4°C with continuous shaking. DFPCs preparedfrom such procedures were defined as ACSDs.

Invitro corneal stromal cell lysis assay

Theanterior, middle and deep stromal lamellar tissues were digested separatelyin 2% collagenase IV in DMEM for 16 h at 37°C. Corneal stromal cellswere harvested and cultivated in 100% human serum or DMEM/F12 at 37°C. After 6 and 12 h of incubation, the cells were fixed with 4% paraformaldehyde for 30 min at 4°C and subjected to crystal violet staining [33-35], apoptosis detection or GSIB4 staining as described below.

Apoptosis detection assay

Porcine corneal stromal tissue and stromal cells, after human serum treatment, were subjected to apoptosis detection measurement using terminal deoxynucleotidyl transferase-mediated nick end labeling (TUNEL), staining with the DeadEnd™ Fluorometric TUNEL system according to manufacturer's protocol [36, 37]. Cellular nuclei were stained with DAPI, andapoptotic cellswere examined under laser confocal microscopy (Fluoview 1000, Olympus, Japan).

Xenoantigen α-gal epitopesbinding assay

GSIB4 staining was performed to detect α-gal epitopes (Gala1-3Galb1- 4GlcNAc-R) as previously described [38]. In brief, after fixation, porcine corneal sections and cultured corneal stromal cells were treated with 0.3% hydrogen peroxide for 30 min at room temperature to inhibit endogenous peroxidase, and washed with PBS for 15 min Samples then reacted with Alexa fluor 568 conjugated GSIB4 (5 μg/ml in PBS) for 10 min at room temperature. After 3 washes with PBS for 15 min, the nuclei were counterstained with DAPI. The samples were investigated and photographed with laser confocal microscopy.

DNA fragmentation assay

Porcine corneal stromal cellular DNA extraction and DNA fragmentation assays were performed, as previously reported [39]. After electrophoresis in 0.5% agarose, gels were examined under a UV Transilluminator (Benchtop, UVP, USA) and photographed using a Gel image system (Biocom, Les Ulis, France).

Physical and biomechanical properties analysis

ACSDs and DFPCs (n=5 per assay) with a 10 mm diameter were used. The central part of the tissues was cut into square shape (5 mm×5 mm) for following assays. All steps were conducted at room temperature. The ratio of light transparency, water content, expansion and tensile strength were measured by spectral photometer (DR5000; Hach, CA), the counting cup (VC305; Branluebbe, Germany), electronic scale (AG135; Mettler Toledo, Switzerland) and the precise chest-developer (BAT1000; Aikoh, Japan) respectively, using protocols described previously [1].

Xenotransplantation of DFPCs and ACSDs into rabbits

Adult New Zealand white rabbits (2.0-2.5 kg, 2 months, either gender) were housed and treated in accordance with the ARVO Statement for the Use of Animals in Ophthalmic and Vision Research and according to an experimental procedure approved by the Committee for Animal Research at Xiamen University. All rabbits were anesthetized with intraperitoneal pentobarbital sodium (50 mg/kg) and topical 0.5% proparacaine hydrochloride. The operation site was disinfected with 0.5% povidone iodine. All surgeries were done under an operating microscope (VISU 150, Carl Zeiss, Germany) by the same investigator. After the operation, erythromycin ophthalmic ointment (Sanyi, China) was applied. In addition, norfloxacin eye drops (Wujing, China) were instilled three times a day during the week following the surgery.

To evaluate the histocompatibility of porcine corneal lamellar tissue, ACSDs (6 mm in diameter) were implanted into the mid-depth corneal stromal pocket (n=4) and anterior chamber

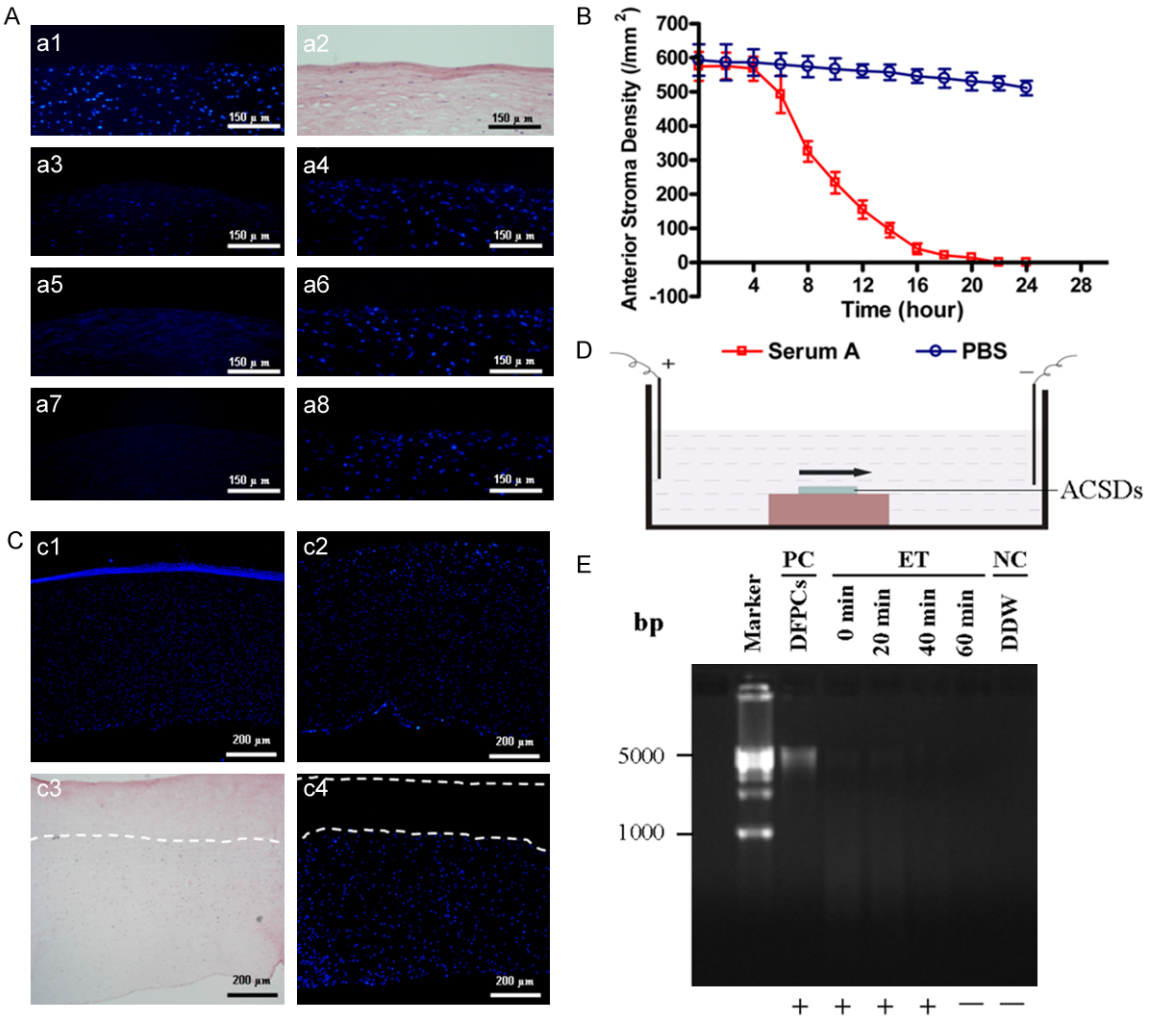

Figure 1. The effect of decellularization using human serum in porcine anterior corneal stroma (PC: positive control; NC: negative control; ET: electrophoresis time; DDW: double distilled water). (A) DAPI (a1) and H&E (a2) staining images of DFPCs. DAPI (blue) staining showed few cellular nuclei in the corneal anterior stroma of the human serum-group at hours 8 (a3), 16 (a5) and 24 (a7) whereas many cellular nuclei were observed in the corneal stroma at the same time points at its corresponding controls (a4, a6, a8). (B) The time course of the numbers of cellular nuclei per mm^2 of the central cornea stroma in both serum and PBS groups. (n=4, **P*<0.05 vs. PBS). (C) DAPI (c1, c2, c4) and H&E (c3) staining images presented the thickness of decellularization in stroma layer after 24 hat 37 °C in PBS (c2)/human serum (c3, c4) with fresh porcine stroma compared to the native porcine cornea (c1). (D) Schematic drawing of the electrophoresis method. (E) DNA extraction and DNA fragmentation assays showed 24 h after serum soaking and 60 min electrophoresis,the remnant DNA material was entirely removed from the DFPCs.

(n=4) of rabbits. To determine the feasibility of ACSDs for lamellar keratoplasty, about 300 mm thickness of the anterior corneal lamellar tissue was removed with a 6.5 mm trephine on the right eye of 18 rabbits. DFPCs (n=9) and ACSDs (n=9) were implanted into the corneal defects, respectively. The rabbits were examined and photographed with slit lamp microscopy weekly after surgery. After different durations of up to 8 weeks, the rabbits were sacrificed and the eyes were enucleated and examined histologically.

Postoperative observation

In vivo confocal microscopy of the rabbit cornea was conducted after lamellar keratoplasty using Heidelberg retina tomograph IIIrostock corneal module (HRT-III RCM, Heidelberg Engineering GmbH, Germany) by the same experienced investigator. Central corneal thickness and the ingrowth of nerve, vessel and stromal cells were determined as previously described [40]. The ratio of corneal light transparency of the transplant area (6 mm in diameter) was

evaluated using a spectral photometer, andthe absorbance was measured by a microplate reader (ELX800, BIO-TEK Corporation, USA). All the rabbits included in the study underwent a thorough ophthalmic evaluation or measurement, including slit-lamp microscopy examination of the anterior segment, and evaluation of the tear film breakup time (TFBUT), tear secretion, using Schirmer I test (ST) under local anesthetic, and corneal surface re-epithelization ratio using fluorescein staining with the criterion according to the van Bijsterveld method [41].

Electron microscopy examination

ACSDs before (n=4) and after (n=3) transplantation were fixed with 2.5% glutaraldehyde in 0.1 M phosphate buffer (pH 7.4), postfixed with osmium tetroxide in 0.1 M phosphate buffer, embedded in Spurr'sresin, and cut into 60 nm sections with an ultramicrotome. The sections were stained with aqueous uranyl acetate and lead citrate and examined under a transmission electron microscope (JEM2100HC; Electronics Co., Ltd, Japan).

Histological examinationand immunofluorescence staining

Samples after different treatment were embedded in OCT, cryostat sections (6 μm) were fixed in acetone for 10 min at -20°C, H&E staining or immunofluorescence staining (primary antibodies: vimentin, 1:50 and α-SMA, 1:100) and DAPI staining were performed as described in our previous studies [42-44]. Sections were observed under a light microscope and Nikon Eclipse epi-fluorescence microscope (TE-200-0U, Nikon, Japan) and photographed.

Data analysis and statistical analysis

For analysis of residual cellular nuclei, apoptotic cell ratio, epithelial cell count and re-epithelization ratio, images from sections were processed using Image Pro Plus V6.0 (Media Cybernetics, Silver Spring, USA). Residual cellular nuclei and apoptotic cells in cornea tissues were counted in a 1 mm^2 area of stroma in each section; three sections from each sample were counted.

Summary data were reported as means ± SD. The numbers of DAPI-positive cellular nuclei, GSIB4-positive cells and apoptotic cells were analyzed using repeated measurements of analysis of variance (ANOVA) followed by the Bonferroni post hoc comparison. Group means were analyzed using the student t-test, where $P<0.05$ was considered statistically significant. Statistical analyses were conducted with GraphPad Prismfor Windows, ver. 5.00 (GraphPad Software. Inc, USA).

Results

Fresh human serum combined with electrophoresis can decellularizeanterior stromaofporcine cornea

To assess the effect of human serum on porcine corneal stromal cells, central porcine corneas, after removal of epithelium and endothelium, were incubated in fresh human serum for different time durations. DAPI and H&E staining revealed evenly distributed nuclei of stromal cells before incubation (**Figure 1Aa1**, **1Aa2**). Intriguingly, nuclei staining in the anterior stroma gradually decreased as the incubation time in human serum increased from 8 h to 16 h (**Figure 1Aa3**, **1Aa5**), and was diminished after 24 hours (**Figure 1Aa7**). However, nuclear staining remained constant at all the time points in the PBS treated group (**Figure 1Aa4**, **1Aa6**, **1Aa8**). Cell nuclear counting confirmed a significant decrease of nuclear numbers in the anterior stroma from 8 h to 24 h in serum treated cornea compared with that of PBS treated cornea (**Figure 1B**). Low power images demonstrated that there was no obvious decline of stromal nuclear density after PBS treatment for 24 h (**Figure 1Cc2**), compared with intact fresh porcine cornea (**Figure 1Cc1**). In contrast, H&E (**Figure 1Cc3**) and DAPI (**Figure 1Cc4**) staining showed that nuclei loss was confined to the depth of 250 to 400 μmin the anterior corneal stromaafter incubation in human serum for 24 h.

To further confirm the decellularization effect of human serum on porcine corneal stroma, we treated anterior and posterior stromal lamellar tissue separately with human serum for 24 h, and the results showed that nuclei loss only happened in the anterior stroma (data not shown). To remove further the hereditary material, electrophoresis (schematic drawing shown in **Figure 1D**) was conducted on DFPC after serum or PBS treatment for different time durations up to 1 h at 4°C. Subsequently, DNA from

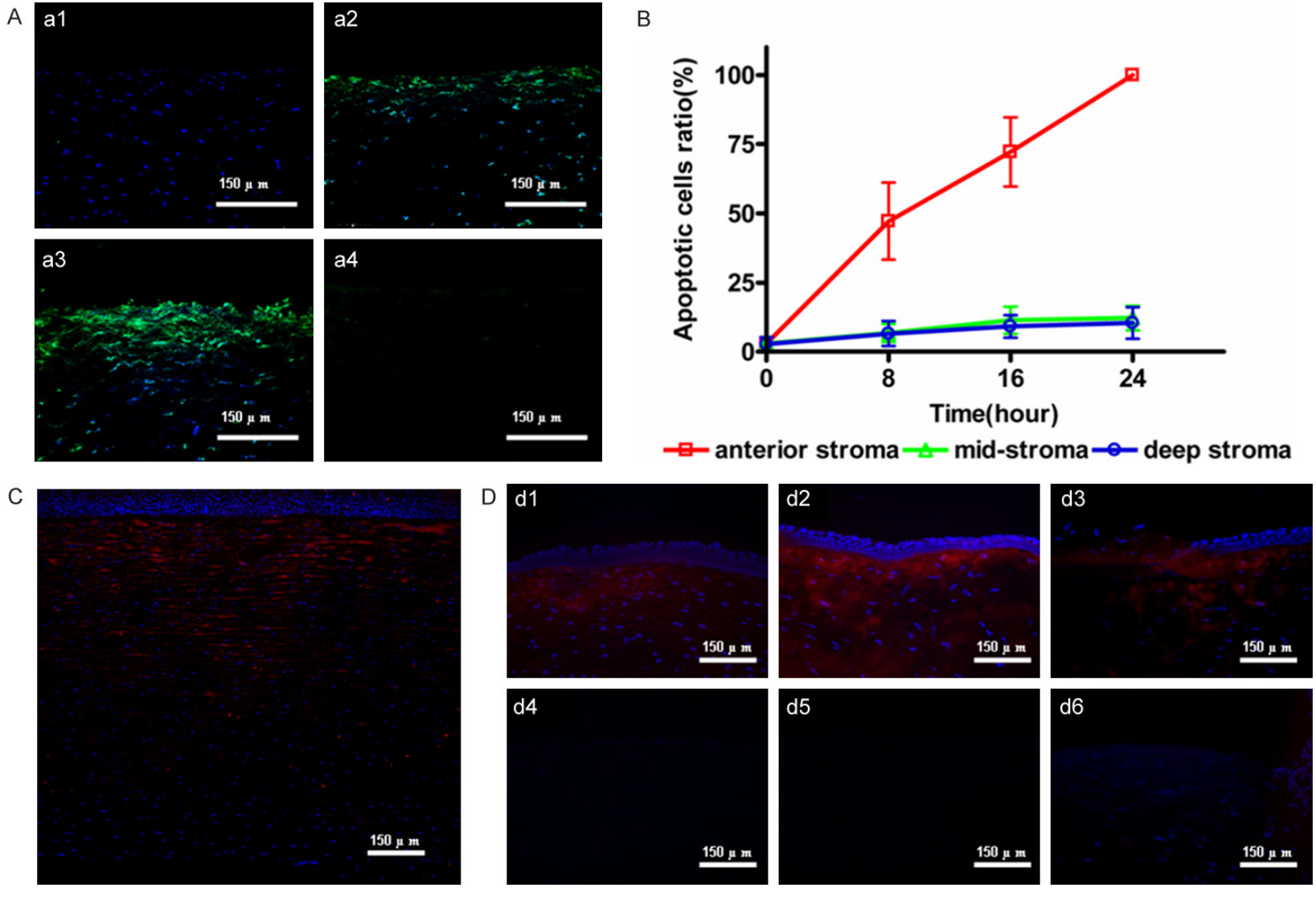
A
a1
a2
a3
a4
150 μm
B
Apoptotic cells ratio(%)
100
75
50
25
0
0
8
16
24
Time(hour)
anterior stroma
mid-stroma
deep stroma
C
D
d1
d2
d3
d4
d5
d6

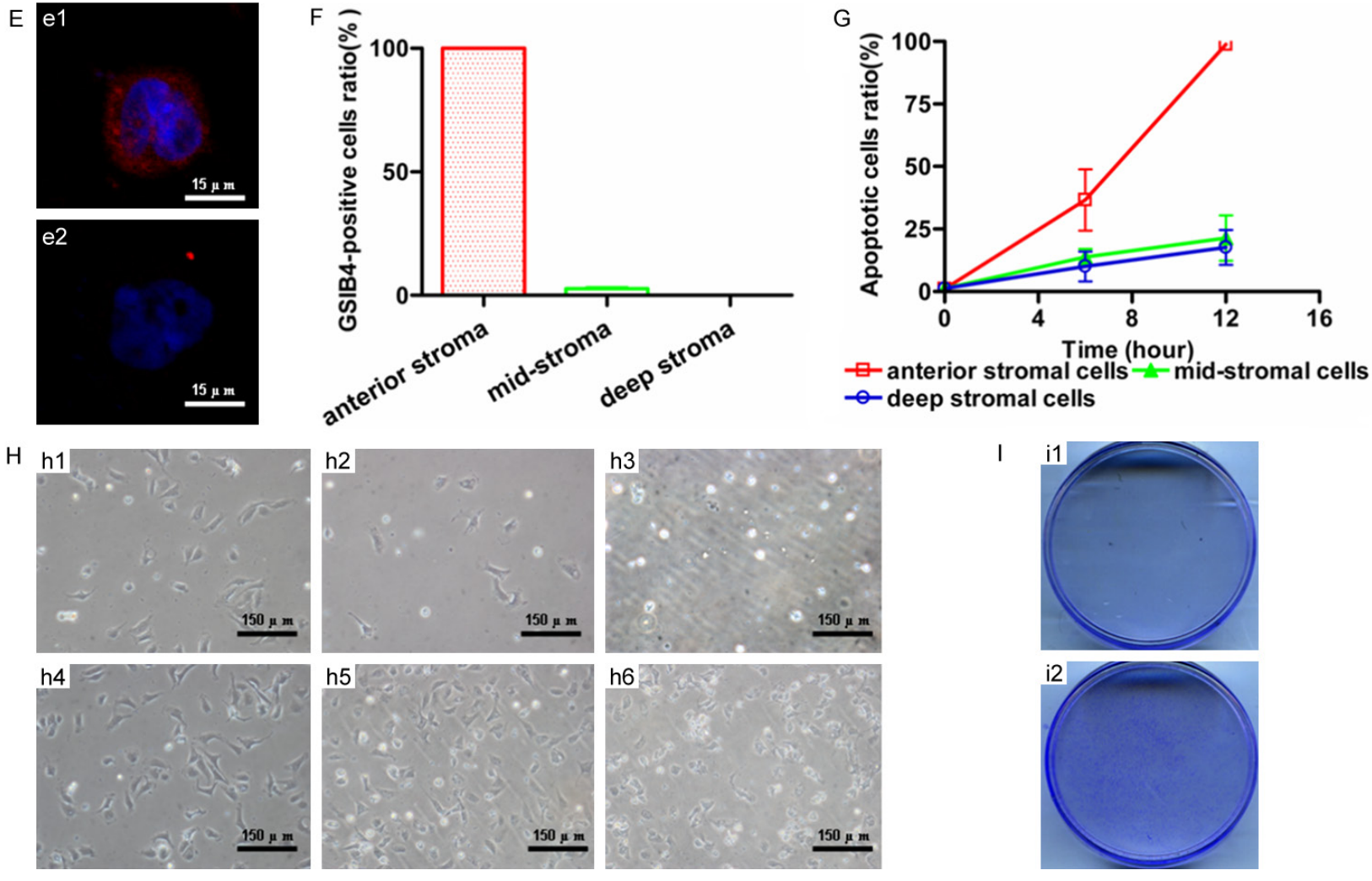

Figure 2. The mechanism of decellularization in porcine anterior corneal stroma using human serum. The TUNEL assay (A) and apoptotic cells measurement (B) showed few apoptotic cells (Green) in the middle and deep corneal stroma whereas many apoptotic cells were observed in the anterior stroma of DFPCs at the same time point. (C, D) Strong GSIB4 staining was present in the anterior stroma of the central cornea (C, Dd1), peripheral cornea (Dd2), and limbus (Dd3). While there was no GSIB4 staining in the anterior stroma of the whole cornea (Dd4-d6) after 24 hr's treatment with human serum. (E) Single cell staining showed strong GSIB4 staining in anterior corneal stromal cells (Ee1), and weak staining in the middle and deep corneal stromal cells (Ee2). Cell counting confirmed almost all GSIB4 positive cells were from anterior stroma, while very few positive cells were from middle and deep stroma (F). TUNEL assay showed mild increase of apoptosis in middle and deep corneal stromal cells, and a dramatic increase of apoptosis in anterior stromal cells when incubated with human serum for different durations (G). Cell photograph (H) and crystal violet staining (I) also showed reduced density of anterior stromal cells (Hh1-3, Ii1), while increased density of middle and deep stromal cells (Hh4-6, Ii2) when incubated with human serum for different durations (Hh1, Hh4: 0 h; Hh2, Hh5: 6 h; Hh3, Hh6, Ii1, Ii2: 12 h).

the lamellar corneal tissue was extracted for agarose gel electrophoresis (100 mg sample, n=4). The results revealed that the trace remnants of DNA in stromal tissues after human serum treatment were undetactable after 1 h's electrophoresis (**Figure 1E**).

Human serum decellularization activity on porcine anterior corneal stromal cells is associated with Gal alpha (1, 3) epitopes

To investigate the mechanism of the decellularization effect of human serum on porcine anterior corneal stromal cells, TUNEL assay was conducted to detect apoptosis. The results showed that there was no positive staining in normal porcine corneal stroma before treatment (**Figure 2Aa1**), that positive nuclei dramatically increased when the stroma tissues were incubated with human serum for 8 and 16 h (**Figure 2Aa2**, **2Aa3**, respectively), and that there was no nuclei staining after human serum treatment for 24 h (**Figure 2Aa4**). In contrast, there were no obvious apoptotic cells in the corneal stroma when DFPCs were treated with PBS for 24 h (data not shown). Apoptotic cell counting demonstrated that the majority of apoptotic cells resided in the anterior stroma while only sporadic apoptotic cells were observed in the middle and posterior parts of the stroma (**Figure 2B**).

To determine whether α-galepitopes were related to this decellularizing procedure, we measured thedistribution of α-gal epitopes in porcinecorneal tissue and in corneal stromal cells using GSIB4 staining. As expected, strong GSIB4 staining was present in the anterior stroma of the central (**Figure 2Dd1**) and peripheral (**Figure 2Dd2**) cornea and limbal stroma (**Figure 2Dd3**), while weak staining was found in the middle and deep corneal stroma (**Figure 2C**). GSIB4 staining vanished in the porcine corneal stroma that was treated with human serum for 24 h (**Figure 2Dd4-d6**), but remained in the stroma treated with PBS (data not shown). Xenoantigen α-gal epitopes binding assay on single stromal cells further confirmed that all the anterior stromal cells expressed α-gal (**Figure 2Ee1**), while few positive cells were observed from the middle and deep stroma (**Figure 2Ee2**, **2F**). Stromal cells harvested from the anterior, middle, and deep native corneal stroma were further incubated with human serum or DMEM basal medium for 12 h. The results showed that the cells from the anterior stroma gradually shrunk and detached from the culture dish (**Figure 2Hh1-h3**), while the cells from deep stroma spread out and attached well in human serum (**Figure 2Hh4-h6**). Crystal violet staining demonstrated cell density differences between cells from the anterior stroma (**Figure 2Ii1**) and the deep stroma (**Figure 2Ii2**) after 12 h's incubation. TUNEL assay confirmed that the anterior stromal cells went into apoptosis within 12 h's incubation with human serum, while the stromal cells from the middle and deep stroma showed little apoptosis (**Figure 2G**).

The optical, biomechanical propertiesand ultrastructure between ACSDs and DFPCs

ACSDs remained transparent after the decellularization procedure (**Figure 3A**). Evaluation of normal porcine cornea and ACSDs with TEM demonstrated that the decellularized stroma had structural similarity to native tissues without signs of disruption or degradation of collagen fibrils (**Figure 3B-D**). The collagen fibril spacing/diameter of ACSDs was 25.9±2.6 nm/28.3±2.2 nm, close to that of native porcine cornea (24.4±6.9 nm/28.2±1.6 nm); there were no significant differences ($P>0.05$). Assessment of biomechanical properties, such as ratio of expansion, water content, light transparency, and tensile strength, demonstrated that ACSDs were identical to DFPCs, without significant difference ($P>0.05$) (**Figure 3Ee1-e4**, respectively).

Good histocompatibility of ACSDs in rabbit corneal stromal pockets and anterior chamber

To examine the compatibility of ACSDs in vivo, corneal pocketand anterior chamber implantation assays were applied. The results showed that ACSDs remained transparent in the corneal stromal pocket (**Figure 3F**), while they became opaque in the anterior chamberafter 2 months of transplantation (**Figure 3H**). Histological examination of the ACSDs and recipient corneas demonstrated that the transplanted ACSDs remained in the rabbit stromal pocket and there were few cells infiltrated into the ACSDs (**Figure 3G**), while there was no cell infiltration in ACSDs that transplanted in theanterior chamber (**Figure 3I**).

Porcine ACSDscan be substitute of corneal lamellar tissue for rabbit LKP

To investigate further the efficacy of ACSDs in xenotransplantation, we used the rabbit LKP

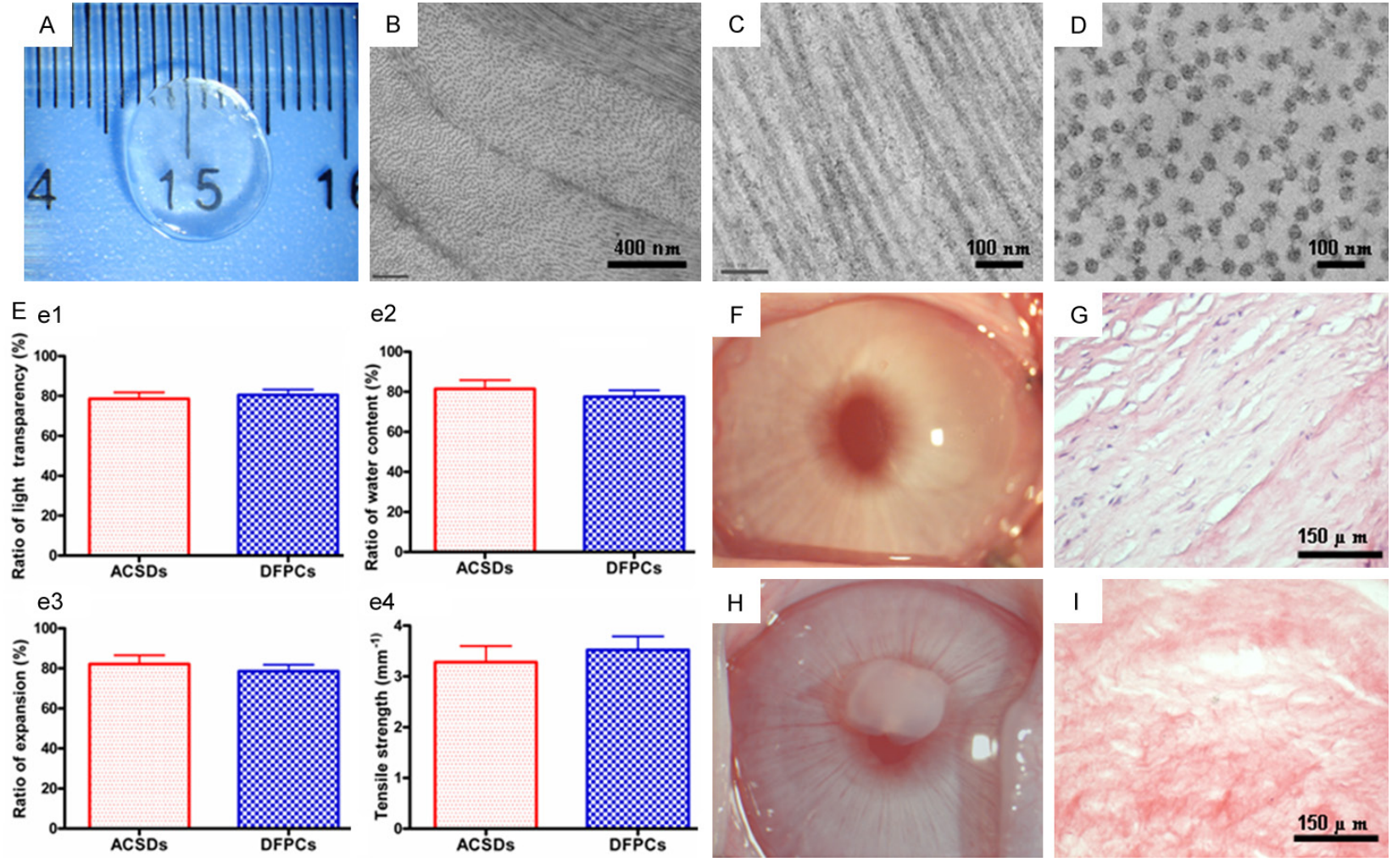

Figure 3. Biomechanical properties and histocompatibilityof decellularized ASCDs in vivo and in vitro. ACSDs showed high transparency under dissecting microscope (A), uniform stroma lamella (B) and collagen fibril arrangement (C, D) under TEM. (E) ACSDs showed similar optical, physical and biomechanical properties compared withDFPCs based on ratio of light transparency (Ee1), water content (Ee2), expansion (Ee3) and tensile strength (Ee4) detection (n=5, $p>0.05$). ACSDs in rabbit corneal stroma pockets remained transparent 2 months after surgery (F), H&E staining showed no inflammatory cell infiltration and no blood vessel formation (G). ACSDs in rabbit anterior chambers for 2 months did not cause inflammation (H), H&E staining showed ACSDs remained acellular (I).

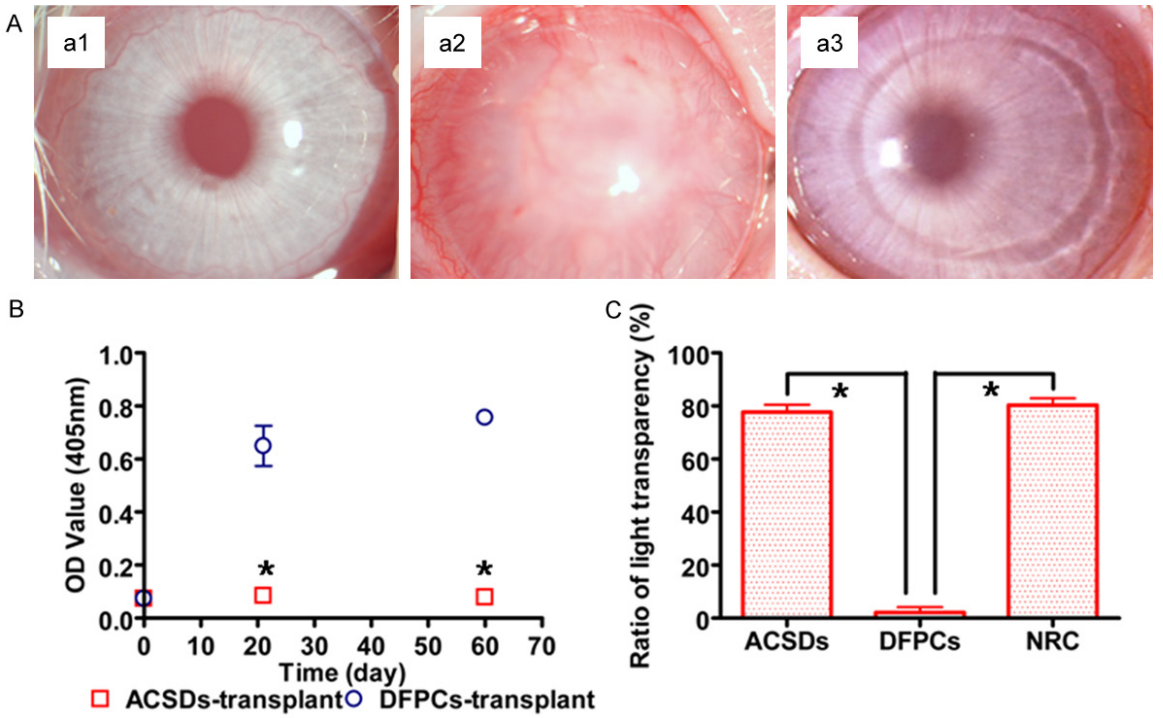

Figure 4. The transparency of the ASCD grafts after LKP. (A) Slit lamp images showed pre-operation, normal rabbit cornea (Aa1) and regenerated cornea after DFPCs (Aa2) and ACSDs (Aa3) transplantation for 2 months. The OD value remained at a low level in ACSDs transplanted cornea within 2 months, while there was a significant increase in DFPCs transplanted cornea at 3 weeks and 2 months after surgery (B). Ratio of light transparency examination at 2 months showed a dramatic decrease in DFPCs transplanted cornea, while ACSDs transplanted cornea displayed similar transparency with normal rabbit cornea (C).

model, as described above. Two months after transplantation, inflammatory responses, including corneal opacification and neovascularization in the peripheral regions, were noted in the DFPCs group. Superficial blood vessels grew into the central region of the graft and the transparency of DFPCs grafts reduced (**Figure 4Aa2**). In contrast, no blood vessels were noted in ACSDs transplantation 2 months post-operatively, and the cornea remained transparent in all of the rabbits with ACSDs graft (**Figure 4Aa3**). Three weeks and 2 months after LKP, the corneas with DFPCs showed much higher OD values than did the corneas with ACSDs ($P<0.05$, **Figure 4B**). Accordingly, corneas with ACSDs showed ratio of light transparencies similar to normal cornea (**Figure 4Aa1**), much higher than that of corneas with DFPCs ($P>0.05$, **Figure 4C**).

In order to investigate the remodeling of ACSDs after LKP in rabbits, in vivo confocal laser scanning microscopy was performed 2 months after transplantation. In normal rabbit cornea, confocal microscopy results demonstrated stratified epithelium (**Figure 5Aa1**), compact stroma with keratocytes (**Figure 5Aa2**), anterior stroma innervation (**Figure 5Aa3**), branching nerve bundles (**Figure 5Aa4**) andintact and regular endothelium (**Figure 5Aa5**). Large quantities of inflammatory cells and new blood vessels were present in the graft tissues in the DFPCs group (**Figure 5Ab1-b5**), whereas few keratocytes without new vessels and nerves were tracked in the stroma in the ACSDs group (**Figure 5Ac1-c5**). The central cornea thickness of the DFPCs group was greater than that of the ACSDs group at 2 weeks and 3 weeks, while there was no significant difference 2 months after surgery ($P<0.05$, **Figure 5B**). The TFBUT in the DFPCs group was significantly shorter than that of the ACSDs group ($P<0.05$, **Figure 5C**), while there were no significant changes in the re-epithelization ratio and Schirmer I test (ST) between the two groups ($P>0.05$, **Figure 5D**, **5E**).

In vivo remodeling and wound healing process of ACSDsin the rabbit LKP model

To detect the wound healing processof ACSDs in the rabbit LKP model, H&E staining and

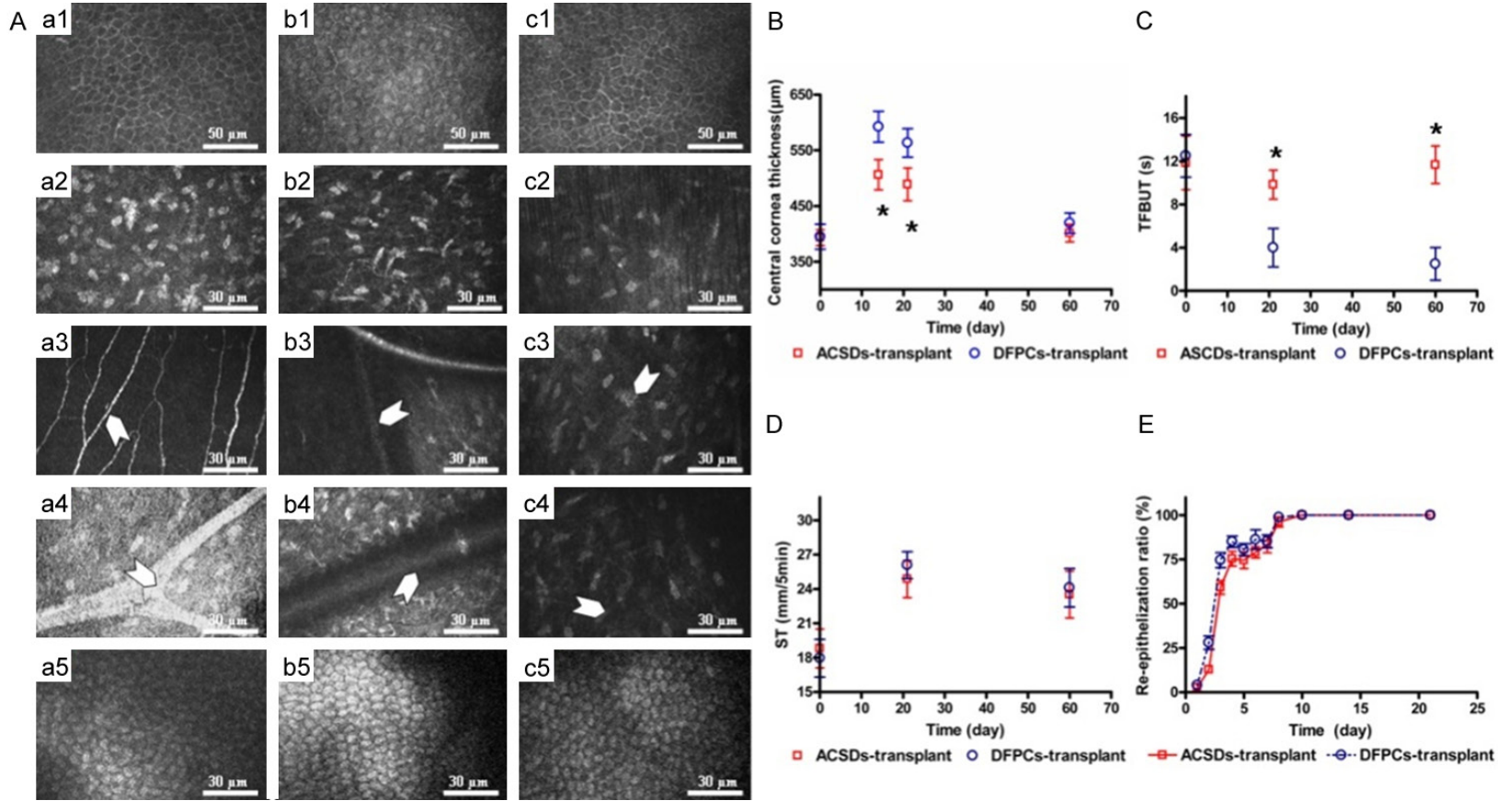

Figure 5. In vivo confocal microscopic images (A) and post-operation observation (B, C, D, E) after LKPin different groups. Confocal microscopy of normal rabbit cornea (a1-a5), LKP with DFPCs (b1-b5), and LKP with ACSDs (c1-c5). The images demonstrated stratified epithelium (a1), compact stroma with keratocytes (a2), anterior stroma innervations (a3), branching nerve bundles (a4) andintact and regular endothelium (a5) in normal rabbit cornea. Two months after LKP, a large number of inflammatory cells (b2) with new vessels (b4) were present in the graft tissues in the DFPCs group, whereas few keratocytes without new vessels and nerves were tracked in the stroma in ACSDs group (c2-c4), and there was no significant difference in the corneal epithelium (b1, c1) and endothelium (b5, c5). The central cornea thickness in the DFPCs group was greater than that of the ACSDs group at 2 weeks and 3 weeks, while there was no significant difference 2 months after surgery (*P<0.05, B). The TFBUT in the DFPCs group was significantly shorter than that of the ACSDs group (*P<0.05, C). There were no significant differences between the two groups in re-epithelization ratio (D) or Schirmer I test (E), (P>0.05, respectively).

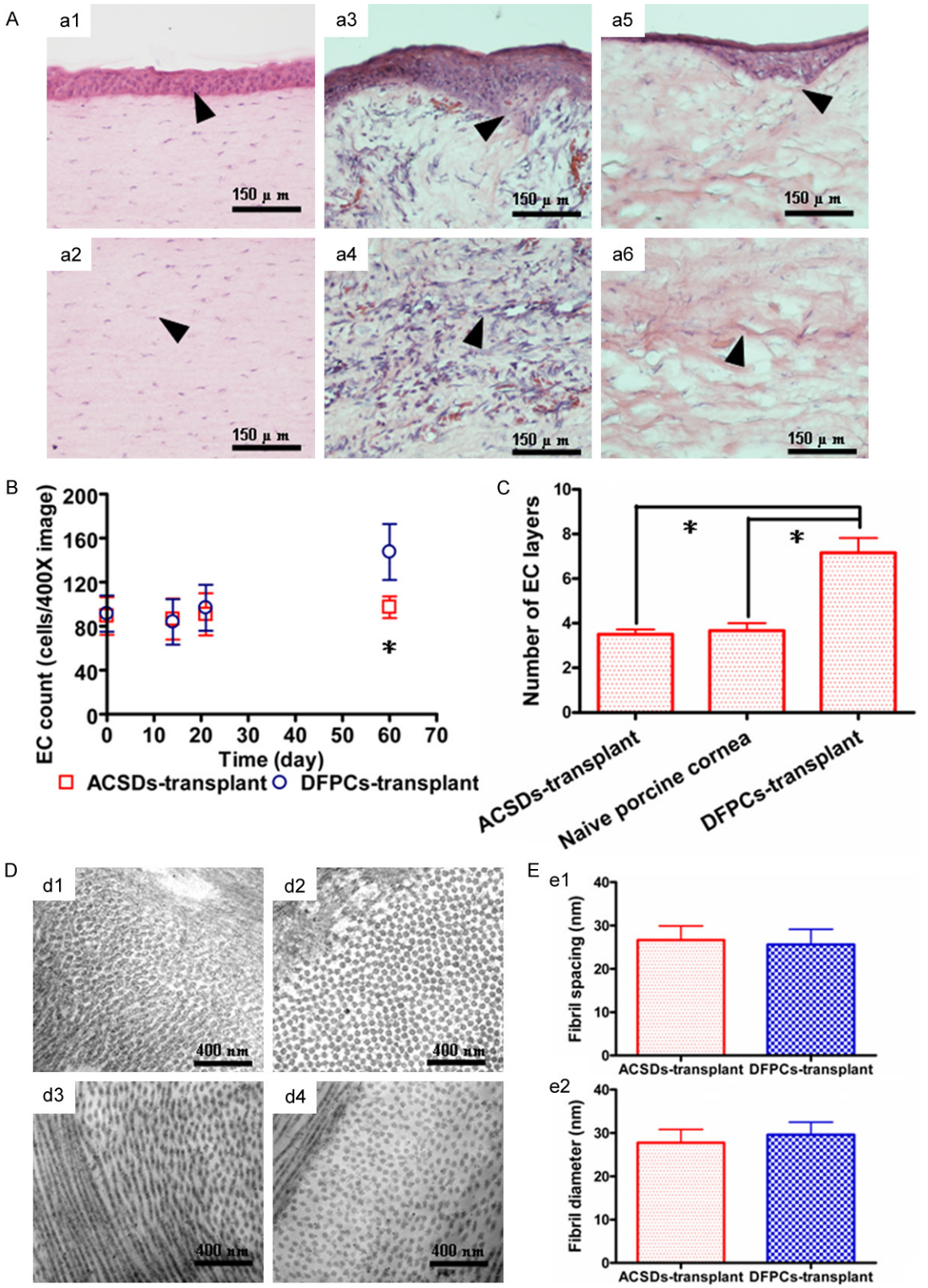

Figure 6. Thewound healing (A-C) and ultrastructure (D) of the grafts after LKP. (A) Normal rabbit cornea showed regular epithelium, anterior stroma (a1), and middle stroma (a2). The wound junction between graft and recipient bed in DFPCs transplantation showed increased epithelial stratification (arrowhead, a3), anterior and middle stroma cell infiltration and new blood vessel formation (arrowhead, a4) 2 months after surgery. However, in ACSDs transplantation, the wound junction showed less epithelial stratification (arrowhead, a5), very few cell infiltrations

(a5), and no blood vessel formation (a6). Epithelial cell number (B) and cell layer (C) counting showed significant increase in DFPCs transplantation compared with ACSDs transplantation 2 months post-operation (*P<0.05). (D) The collagen fiber arrangementin the DFPCs (d1, d2) and ACSDs (d3, d4) at 3 weeks (d1, d3) and 2 months (d2, d4) after surgery. (E) The collagen fibril spacing (e1)/diameter (e2) of ACSDs was 26.62±2.88 nm/27.46±2.55 nm, close to that of DFPCs grafts (25.74±3.22 nm/29.58±2.31 nm), and showed no significant difference (P>0.05).

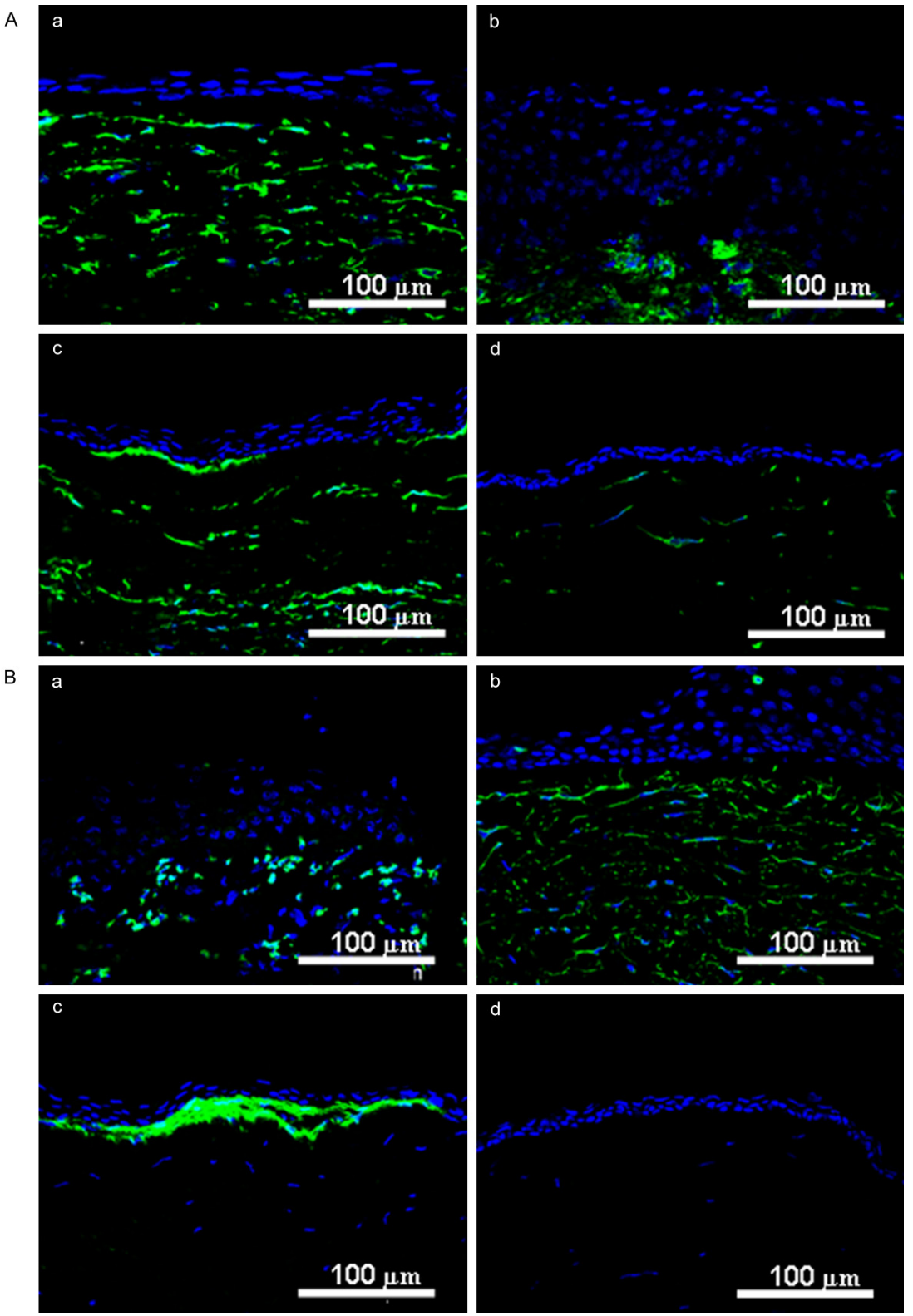

Figure 7. Corneal stroma remodeling after ACSDs and DFPCs transplantation. Three weeks after DFPCs and ACSDs transplantation, there was strong expression of vimentin in both DFPCs (Aa) and ACSDs (Ac). Two months after surgery, vimentin expressed irregularly in DFPCs (Ab), while expressed weakly in ACSDs (Ad). Three weeks after surgery, α-SMA was highly expressed in the stroma of DFPCs (Ba) and the sub-epithelial superficial stroma of ACSDs (Bc). Two months after surgery, α-SMA expression remained in the whole stroma of DFPCs (Bb), while it was negative in ACSDs (Bd).

transmission electron microscopy were applied. Similar to the native rabbit cornea (**Figure 6Aa1**, **6Aa2**), H&E staining showed 3 to 4 layers of epithelial cells covering the graft with no visible boundary between the ACSD graft and the recipient bed, and there were many cells that had migrated into the graft tissue 2 months after transplantation (**Figure 6Aa5**, **6Aa6**). In DFPCs grafts, however, the epithelium was much thicker and there was prominent cell infiltration, as well as new blood vessel formation (**Figure 6Aa3**, **6Aa4**). Epithelial cell counting confirmed more epithelial cells (**Figure 6B**) and greater epithelial stratification in the central area of DFPCs grafts 2 months post-operation (**Figure 6C**). Before the operation, normal rabbit cornea had uniform collagen spacing (data not shown). Three weeks after transplantation, the collagen fibril diameter was invariable andthe collagen fibril spacing was decreased (**Figure 6Dd1**, **6Dd3**) 2 months after transplantation, however, the collagen fibril spacing/diameter of ACSDs was 26.62±2.88 nm/27.46±2.55 nm (**Figure 6Dd2**), close to that of the DFPCs grafts (25.74±3.22 nm/29.58±2.31 nm) (**Figure 6Dd4**); they were not significantly different ($P > 0.05$, **Figure 6Ee1**, **6Ee2**).

To investigate further the wound healing process of rabbit LKP using ACSDs and DFPCs, immunostaining of vimentin and α-SMA were performed 3 weeks and 2 months after surgery. In normal porcine cornea, vimentin was expressed in all the corneal stromal cells while α-SMA was negative (data not shown). Three weeks after surgery, there was a strong expression of vimentin in both DFPCs (**Figure 7Aa**) and ACSDs (**Figure 7Ac**). Two months after surgery, vimentin expressed irregularly in DFPCs (**Figure 7Ab**), and weakly in ACSDs (**Figure 7Ad**). Three weeks after surgery, α-SMA was highly expressed in the stroma of DFPCs (**Figure 7Ba**) and in the sub-epithelial superficial stroma of ACSDs (**Figure 7Bc**). Two months after surgery, α-SMA expression remained in the whole stroma of DFPCs (**Figure 7Bb**), while this expression was negative in ACSDs (**Figure 7Bd**).

Discussion

Our study, for the first time, demonstrated that short term incubation with human serum and additional electrophoresiscan effectively decellularize and remove α-gal epitopes in the anterior lamellar of porcine corneal stroma without reducing corneal transparency. Compared with previously reported methods, our method is relatively mild and simple, without introducing enzymes or other noxious substances into the cornea. This method, therefore, may indicate clinical significance in generating corneal lamella tissue for lamella keratoplasty.

Our results showed that the decellularization activity of human serum on porcine corneal stromal cells occurs through inducing apoptosis of the keratocytes. TUNEL assay revealed apoptotic cells after 8hr's incubation, with positive staining confined in the nuclei (**Figure 2Aa2**). Interestingly, after 16 hr's incubation, positive staining in the anterior stroma diffused into the matrix (**Figure 2Aa3**), indicating that there was cellular and nuclear membrane lysis during the procedure. As a result, the fragmented DNA was released into the extracellular matrix. Our study further confirmed that the apoptotic cells were mainly located in the anterior stroma, while very few were evident in the middle or deep stroma (**Figure 2B**). This prompted us to hypothesize that there is heterogeneity among the keratocytes between different portions of the cornea. Indeed, similar to previous studies [25, 27], we found that α-gal epitopes were mainly expressed in the anterior stroma, and that the expression pattern was well correlated with keratocyte apoptosis. We then performed in vitro cell lysis assay, and found that human serum can induce apoptosis of keratocytes only from anterior stroma, and not from middle or deep stroma (**Figure 2G**). Thus, our data indicated that the decellularization activity of human serum on porcine corneal keratocytes was most likely mediated by α-galepitopes. Since cornea is an avascular tissue, the keratocyte apoptosis is presumed to beantibody-

dependent cell-mediated destruction but not complement-mediated destruction.

Our study also clearly showed that porcine corneal stroma was deprived of GSIB4 staining after human serum treatment, indicating that α-gal epitopes may be removed from the stroma along with other components of the keratocytes [45, 46]. α-gal epitopes also can be removed by incubation with recombinant α-galactosidase [47]; however, α-galactosidase treatment alone will not eliminate keratocytes, which can produce new α-gal epitopes after xenotransplantation. The α-galactosidase treatment, therefore, is rendered inapplicable. The possibility that α-gal epitopes combined with anti-Gal antibodies from human serum and blocked the binding sites of GSIB4 cannot be ruled out [22, 48]. Even if this is the case, however, it may also be helpful in preventing xenogenic rejection through blocking α-gal epitope after transplantation.

In order to generate acellular corneal stromal tissue for clinical application, the manipulation procedure should be as simple as possible, while maintaining the architecture and function of the donor tissue. In previous studies, the decellularization procedure normally took 3 to 7 days and multiple steps [1, 2], while the whole procedure can be completed within 2 days using this study's protocol. The porcine corneal lamella tissue generated from this study's method displayed similar optical, biomechanical propertiesand ultrastructure to native porcine cornea, and showed high biocompatibility when transplanted into rabbit corneal stromal pockets and anterior chambers.

To prove whether such lamella tissue can be used for corneal reconstruction, we performed LKP on rabbits. Postoperative clinical assessments of corneal transparency, thickness, re-epithelization, and tear film characteristics, such as tear film break-up time and tear secretion, demonstrated encouraging outcomes. Moreover, in vivo confocal laser scanning microscopyshowed that stromal cells and epithelial cells were evident in ACSDs without reducing corneal transparency or inducing rejection, two months postoperatively (**Figure 5A**). Immunostaining with vimentin showed that there was cell re-population in the lamella tissue 3 weeks after transplantation, and that the cells became more organized at 2 months post-operation (**Figure 7A**). Further study is needed to clarify whether the vimentin positive cells are all keratocytes migrated from surrounding recipient tissue or whether they include other cell types [49]. α-SMA staining revealed excessive wound healing in LKP with DFPCs, even 2 months after surgery (**Figure 7Ba**, **7Bb**). In the ASCDs transplantation group, we found α-SMA expression in superficial stroma 3 weeks after surgery, indicating that there was myofibroblast differentiation during the early stage of tissue remodeling and cell re-population, while those α-SMA positive cells diminished after 2 months [50, 51]. Further studies are also necessary to evaluate the long-term nerve recovery of this biomaterial in the LKP model and its effect in the Macaca rhesus model before clinical application.

In conclusion, our method of decellularization using human serum and electrophoresis can remove porcine corneal anterior stromal cells and α-gal epitopes. Acellular porcine corneal stromal tissue ACSDs have a good histocompatibility, similar optical and biophysical propertiesto native porcine cornea and can be used as a corneal stroma equivalentin xenotransplantation. This novel method may be valuable for decellularizing the corneal stroma for clinical application by using patient serum and full-scale production, using purified anti-Galantibodies. ACSDs may serve as a safe and general bio-engineered cornea substrate for future application in the biomaterial realm. The results of this study may have broader implications for the field of biological tissue engineering, providing new insight into antigen/cellular rejection and hereditary materialand α-gal deprivation in other engineered organ or tissue systems designed for xerotransplantation; both are major goalsin tissue engineering.

Acknowledgements

We thank Dr. Lelei Chen, Yao Yu and Juan Li for their generous support in clinic study andZhiyuan Li, Xiaoling Wu and Jiaoyue Hu for their technical support in the experiment. We thank Professor Jianxing Ma for critical review of the project proposal. This study was supported by Grants from The National High Technology Research and Development Program of the Eleventh Five-Year Plan of China (2006AA02A131), the National Natural Science Foundation of China (81160118 and 81400372); Clinical

Medicine Research Special-purpose Foundation of China (L2012052); Jiangxi Province Voyage Project (2014022); Jiangxi province Degree and Postgraduate Education Reform Project (2015); Science and Technology Platform Construction Project of Jiangxi Province (2013116); Youth Science Foundation of Jiangxi Province (20151BAB215016); Technology and Science Foundation of Jiangxi Province (20151BBG-70223); Jiangxi Province Education Department Scientific Research Foundation (GJJ14170); Health Development Planning Commission Science Foundation of Jiangxi Province (20155-154); Scholor Project of Ganjiang River (2015).

Disclosure of conflict of interest

None.

Address correspondence to: Drs. Zuguo Liu and Wei Li, Eye Institute of Xiamen University, 3rd Floor of Chengyi Building, Xiang'annan Road, Xiamen, Fujian 361102, China. Tel: (86) 592-2183761; Fax: (86) 5922183761; E-mail: profzg.liu@aliyun.com (ZGL); profw.li@aliyun.com (WL)

References

[1] Wang H, Zhang Y, Li Z, Wang T, Liu P. Prevalence and causes of corneal blindness. Clin Experiment Ophthalmol 2014; 42: 249-253.

[2] Xu YG, Xu YS, Huang C, Feng Y, Li Y and Wang W. Development of a rabbit corneal equivalent using an acellular corneal matrix of a porcine substrate. Mol Vis 2008; 14: 2180-2189.

[3] Dhamodaran K, Subramani M, Jeyabalan N, Ponnalagu M, Chevour P, Shetty R, Matalia H, Shetty R, Prince SE, Das D. Characterization of ex vivo cultured limbal, conjunctival, and oral mucosal cells: A comparative study with implications in transplantation medicine. Mol Vis 2015; 21: 828-845.

[4] Amano S, Shimomura N, Yokoo S, Araki-Sasaki K, Yamagami S. Decellularizing corneal stroma using N2 gas. Mol Vis 2008; 14: 878-882.

[5] Lin XC, Hui YN, Wang YS, Meng H, Zhang YJ and Jin Y. Lamellar keratoplasty with a graft of lyophilized acellular porcine corneal stroma in the rabbit. Vet Ophthalmol 2008; 11: 61-66.

[6] Griffith M, Osborne R, Munger R, Xiong X, Doillon CJ, Laycock NL, Hakim M, Song Y and Watsky MA. Functional human corneal equivalents constructed from celllines. Science 1999; 286: 2169-2172.

[7] Zieske JD, Mason VS, Wasson ME, Meunier SF, Nolte CJ, Fukai N, Olsen BR and Parenteau NL. Basement membrane assembly and differentiation of cultured corneal cells: importance of culture environment and endothelial cell interaction. Exp Cell Res 1994; 214: 621-33.

[8] Minami Y, Sugihara H and Oono S. Reconstruction of cornea in three-dimensional collagen gel matrix culture. Invest Ophthalmol Vis Sci 1993; 34: 2316-2324.

[9] Brown KD, Low S, Mariappan I, Abberton KM, Short R, Zhang H, Maddileti S, Sangwan V, Steele D, Daniell M. Plasma polymer-coated contact lenses for the culture and transfer of corneal epithelial cells in the treatment of limbal stem cell deficiency. Tissue Eng Part A 2014; 20: 646-655.

[10] Liu W, Deng C, McLaughlin CR, Fagerholm P, Lagali NS, Heyne B, Scaiano JC, Watsky MA, Kato Y, Munger R, Shinozaki N, Li F and Griffith M. Collagen-phosphorylcholine interpenetrating network hydrogels as corneal substitutes. Biomaterials 2009; 30: 1551-1559.

[11] Shah A, Brugnano J, Sun S, Vase A and Orwin E. The Development of a Tissue-Engineered Cornea: Biomaterials and Culture Methods. Pediatr. Res 2008; 63: 535-544.

[12] Merrett K, Fagerholm P, McLaughlin CR, Dravida S, Lagali N, Shinozaki N, Watsky MA, Munger R, Kato Y, Li F, Marmo CJ and Griffith M. Tissue-engineered recombinant human collagen-based corneal substitutes for Implantation: performance of type I versus type III collagen. Invest Ophthalmol Vis Sci 2008; 49: 3887-3894.

[13] Li F, Carlsson D, Lohmann C, Suuronen E, Vascotto S, Kobuch K, Sheardown H, Munger R, Nakamura M and Griffith M. Cellular and nerve regeneration within a biosynthetic extracellular matrix for corneal transplantation. Proc Natl Acad Sci U S A 2003; 100: 15346-51.

[14] Acun A, Hasirci V. Construction of a collagen-based, split-thickness cornea substitute. J Biomater Sci Polym Ed 2014; 25: 1110-1132.

[15] Bongoni AK, Kiermeir D, Denoyelle J, Jenni H, Burlak C, Seebach JD, Vögelin E, Constantinescu MA, RiebenR. Porcine extrahepatic vascular endothelial asialoglycoprotein receptor 1 mediates xenogeneic platelet phagocytosis in vitro and in human-to-pig ex vivo xenoperfusion. Transplantation 2015; 99: 693-701.

[16] Sykes M, D'Apice A and Sandrin M. Position paper of the Ethics Committee of the International Xenotransplantation Association. Transplantation 2004; 78: 1101-1107.

[17] Kampmeier J, Radt B, Birngruber R and Brinkmann R. Thermal and biomechanical parameters of porcine cornea. Cornea 2000; 19: 355-363.

[18] Jay L, Brocas A, Singh K, Kieffer JC, Brunette I, Ozaki T. Determination of porcine corneal layers with high spatial resolution by simultaneous second and third harmonic generation microscopy. Opt Express 2008; 16: 16284-93.

[19] Toledo-Pereyra LH, Lopez-Neblina F. Xenotransplantation: a view to the past and an unrealized promise to the future. ExpClin Transplant 2003; 1: 1-7.
[20] Macher BA, Galili U. The Galalpha1, 3Galbeta1, 4GlcNAc-R (alpha-Gal) epitope: a carbohydrate of unique evolution and clinical relevance. Biochim Biophys Acta 2008; 1780: 75-88.
[21] Galili U, Mandrell RE, Hamadeh RM, Shohet SB, Griffiss JM. Interaction between human natural anti-alpha-galactosyl immunoglobulin G and bacteria of the human flora. Infect Immun 1988; 56: 1730-1737.
[22] Kin T, Nakajima Y, Aomatsu Y, Kanehiro H, Hisanaga M, Ko S, Ohyama T, Nakano H. Humoral human xenoreactivity against isolated pig pancreatic islets. Surg Today 2000; 30: 821-826.
[23] Watier H, Guillaumin JM, Vallee I, Thibault G, Gruel Y, Lebranchu Y, Bardos P. Human NK cell-mediated direct and IgG-dependent cytotoxicity against xenogeneic porcine endothelial cells. TransplImmunol 1996; 4: 293-299.
[24] Galili U. Interaction of the natural anti-Gal antibody with alpha-galactosyl epitopes: a major obstacle for xenotransplantation in humans. Immunol Today 1993; 14: 480-482.
[25] Lee HI, Kim MK, Oh JY, Ko JH, Lee HJ, Wee WR, Lee JH. Gal alpha(1-3)Gal expression of the cornea in vitro, in vivo and in xenotransplantation. Xenotransplantation 2007; 14: 612-618.
[26] Kim MK, Oh JY, Lee HI, Ko JH, Lee HJ, Lee JH, Wee WR. Susceptibility of porcine keratocytes to immune-mediated damage in xeno-related rejection. Transplant Proc 2008; 40: 564-569.
[27] Amano S, Shimomura N, Kaji Y, Ishii K, Yamagami S, Araie M. Antigenicity of porcine cornea as xenograft. Curr Eye Res 2003; 26: 313-318.
[28] Oh JY, Kim MK, Ko JH, Lee HJ, Kim Y, Park CS, Park CG, Kim SJ, Wee WR, Lee JH. Acute cell-mediated rejection in orthotopic pig-to-mouse corneal xenotransplantation. Xenotransplantation 2009; 16: 74-82.
[29] Oh JY, Kim MK, Lee HJ, Ko JH, Wee WR, Lee JH. Processing porcine cornea for biomedical applications. Tissue Eng Part C Methods 2009; 15: 635-645.
[30] Sasaki S, Funamoto S, Hashimoto Y, Kimura T, Honda T, Hattori S, Kobayashi H, Kishida A, Mochizuki M. In vivo evaluation of a novel scaffold for artificial corneas prepared by using ultrahigh hydrostatic pressure to decellularize porcine corneas. Mol Vis 2009; 15: 2022-2028.
[31] Wu Z, Zhou Y, Li N, Huang M, Duan H, Ge J, Xiang P, Wang Z. The use of phospholipase A(2) to prepare acellular porcine corneal stroma as a tissue engineering scaffold. Biomaterials 2009; 30: 3513-3522.
[32] Chang SW, Wang YH and Pang JH. The effects of epithelial viability on stromal keratocyte apoptosis in porcine corneas stored in Optisol-GS. Cornea 2006; 25: 78-84.
[33] Bennet W, Björkland A, Sundberg B, Davies H, Liu J, Holgersson J and Korsgren O. A comparison of fetal and adult porcine islets with regard to Gal alpha (1, 3) Gal expression and the role of human immunoglobulins and complement in islet cell cytotoxicity. Transplantation 2000; 8: 1711-1717.
[34] Shao Y, Quyang L, Zhou Y, Tang J, Tan Y, Liu Q, Lin Z, Yin T, Qiu F, Liu Z. Preparation and physical properties of a novel biocompatible porcine corneal acellularizedmatrix. In Vitro Cell Dev BiolAnim 2010; 46: 600-605.
[35] Zhang Z, Ma JX, Gao G, Li C, Luo L, Zhang M, Yang W, Jiang A, Kuang W, Xu L, Chen J, Liu Z. Plasminogen kringle 5 inhibits alkali-burn-induced corneal neovascularization. Invest Ophthalmol Vis Sci 2005; 46: 4062-4071.
[36] Han Y, Shao Y, Liu T, Qu YL, Li W, Liu Z. Therapeutic effects of topical netrin-4 inhibits corneal neovascularization in alkali-burn rats. PLoS One 2015; 10: e0122951.
[37] Han Y, Shao Y, Lin Z, Qu YL, Wang H, Zhou Y, Chen W, Chen Y, Chen WL, Hu FR, Li W, Liu Z. Netrin-1 simultaneously suppresses corneal inflammation and neovascularization. Invest Ophthalmol Vis Sci 2012; 53: 1285-1295.
[38] Shao Y, Yu Y, Pei CG, Qu Y, Gao GP, Yang JL, Zhou Q, Yang L, Liu QP. The expression and distribution of α-Gal gene in various species ocular surface tissue. Int J Ophthalmol 2012; 5: 543-548.
[39] Zhang Z, Ma JX, Gao G, Li C, Luo L, Zhang M, Yang W, Jiang A, Kuang W, Xu L, Chen J and Liu Z. Plasminogen Kringle 5 Inhibits Alkali-Burn-Induced Corneal Neovascularization. Invest Ophthalmol Vis Sci 2005; 46: 4062-4071.
[40] Villani E, Galimberti D, Viola F, Mapelli C and Ratiglia R. The cornea in Sjogren's syndrome: an in vivo confocal study. Invest Ophthalmol Vis Sci 2007; 48: 2017-22.
[41] van Bijsterveld OP. Diagnostic tests in the sicca syndrome. Arch Ophthalmol 1969; 82: 10-14.
[42] Dong N, Li W, Lin H, Wu H, Li C, Chen W, Qin W, Quyang L, Wang H and Liu Z. Abnormal Epithelial Differentiation and Tear Film Alteration in Pinguecula. Invest Ophthalmol Vis Sci 2009; 6: 2710-2715.
[43] Wang H, Tao T, Tang J, Mao YH, Li W, Peng J, Zhou YP, Zhong JX, Tseng SC, Kawakita T, Zhao YX and Liu ZG. Importin 13 Serves as a Potential Marker for Corneal Epithelial Progenitor Cells. Stem Cells 2009; 27: 2516-2526.
[44] Lin H, Qu Y, Geng Z, Li C, Wu H, Dong N, Liu Z, Li W. Air exposure induced characteristics of dry eye in conjunctival tissue culture. PLoS One 2014; 9: e87368.

[45] Shao Y, Yu Y, Pei CG, Zhou Q, Liu QP, Tan G, Li JM, Gao GP, Yang L. Evaluation of novel decellularizing corneal stroma for cornea tissue engineering applications. Int J Ophthalmol 2012; 5: 415-418.
[46] Cohen D, Miyagawa Y, Mehra R, Lee W, Isse K, Long C, Ayares DL, Cooper DK, Hara H. Distribution of non-gal antigens in pig cornea: relevance to corneal xenotransplantation. Cornea 2014; 33: 390-397.
[47] Stone KR, Ayala G, Goldstein J, Hurst R, Walgenbach A, Galili U. Porcine cartilage transplants in the cynomolgus monkey. III. Transplantation of alpha-galactosidase-treated porcine cartilage. Transplantation 1998; 65: 1577-1583.
[48] Cooper DK. Identification of alpha Gal as the major target for human anti-pig antibodies. Xenotransplantation 2009; 16: 47-49.
[49] Feng Y, Wang W. In vivo confocal microscopic observation of lamellar corneal transplantation in the rabbit using xenogenic acellular corneal scaffolds as a substitute. Chin Med J (Engl) 2015; 128: 933-940.
[50] Almaliotis D, Koliakos G, Papakonstantinou E, Komnenou A, Thomas A, Petrakis S, Nakos I, Gounari E, Karampatakis V. Mesenchymal stem cells improve healing of the cornea after alkali injury. Graefes Arch Clin Exp Ophthalmol 2015; 253: 1121-1135.
[51] Das SK, Gupta I, Cho YK, Zhang X, Uehara H, Muddana SK, Bernhisel AA, Archer B, Ambati BK. Vimentin knockdown decreases corneal opacity. Invest Ophthalmol Vis Sci 2014; 55: 4030-4040.